Graphene Growth by a Metal-Catalyzed Solid-State Transformation of Amorphous Carbon

Julio A. Rodríguez-Manzo,[†] Cuong Pham-Huu,[‡] and Florian Banhart[†,*]

[†]Institut de Physique et Chimie des Matériaux, UMR 7504 CNRS, Université de Strasbourg, 23 rue du Loess, 67034 Strasbourg, France and [‡]Laboratoire des Matériaux Surfaces et Procédés pour la Catalyse, UMR 7515 CNRS, European Laboratory for Catalysis and Surface Sciences, 25 rue Becquerel, 67087 Strasbourg, France

ABSTRACT Single and few-layer graphene is grown by a solid-state transformation of amorphous carbon on a catalytically active metal. The process is carried out and monitored *in situ* in an electron microscope. It is observed that an amorphous carbon film is taken up by Fe, Co, or Ni crystals at temperatures above 600 °C. The nucleation and growth of graphene layers on the metal surfaces happen after the amorphous carbon film has been dissolved. It is shown that the transformation of the energetically less favorable amorphous carbon to the more favorable phase of graphene occurs by diffusion of carbon atoms through the catalytically active metal.

KEYWORDS: graphene synthesis · carbon phases · *in situ* electron microscopy · catalytic transformation

Graphene is one of the most promising materials for future applications in nanoelectronic devices, sensors, electrodes, and composite nanosystems.[1,2] The production of single- or multilayer graphene has been carried out by different techniques, such as exfoliation,[3,4] surface decomposition of carbides,[5,6] chemical vapor deposition (CVD),[7−10] carbon segregation from solid solutions,[11−16] or other chemical methods.[17] In CVD, which has been applied for more than a decade in the growth of carbon nanotubes[18] as well as in solid-state transformations, the basic mechanism is the transformation of carbon from an organic gas or from a solid solution to graphene by the catalytic action of a suitable metal. Of major importance in the growth of high-quality layers of graphene are therefore the role of the catalyst, carbon solubility, and diffusion in or on metal crystals, and the influence of temperature.

Here we show that graphene can be grown in a solid-state transformation of amorphous carbon in the presence of a catalytically active transition metal. This is an alternative route and allows us to study in detail the mechanisms of nucleation and growth of graphene in real time and at high spatial resolution by *in situ* electron microscopy. *In situ* electron microscopy has already been applied in several growth studies of carbon nanotubes[19−26] but only in surface microscopy studies for observing the growth of graphene.[14,27] In the present work, we show how amorphous carbon is taken up by Fe, Co, or Ni crystals and later nucleates as single- or few-layer graphene on the metal surface. It is a solid-state transformation that works in vacuum (no gases are involved) and at moderate temperatures. We make use of the different energies of amorphous and graphenic carbon and apply a metal catalyst as a diffusion channel for carbon atoms that lowers the transformation barrier.

RESULTS

As described in the Experimental Methods section, thin polycrystalline but coherent layers of Fe, Co, Ni, and Cu were deposited onto amorphous carbon films. Annealing of the carbon−metal bilayer samples at temperatures above 400 °C (Co) and 500 °C (Ni) caused the coalescence of metal crystals by migration of the metal crystals and Ostwald ripening.[28] Thus, isolated and thicker metal islands were formed, leaving uncovered areas of the carbon film between them, as shown in a low-magnification overview in Figure 1. At temperatures up to 600 °C, both Co and Ni left the amorphous carbon film unchanged when migrating and coalescing. At higher temperatures, however, the migration of the metal islands during further ripening caused a transformation of the underlying amorphous carbon film to single- or multilayer graphene. The process is shown schematically in Figure 2. Although the ripening effect did also occur for Cu crystals, no transformation of the carbon film by Cu was observed in the whole temperature range.

*Address correspondence to banhart@ipcms.u-strasbg.fr.

Received for review December 14, 2010 and accepted January 12, 2011.

Published online January 20, 2011
10.1021/nn103456z

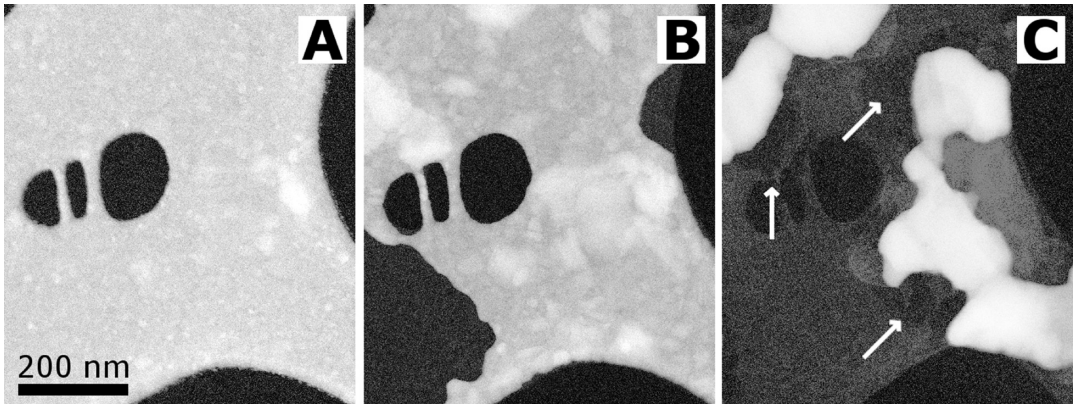

Figure 1. Plan-view scanning transmission electron microscopy (STEM) dark-field images of Ni crystals on an amorphous carbon film at 400 °C (A), 600 °C (B), and 720 °C (C). (A) At 400 °C, the coherent polycrystalline Ni film (bright) covers the C substrate entirely; holes in the C film appear black. (B) At 600 °C, ripening of the metal crystals starts and uncovers areas of the amorphous carbon film (light gray contrast). (C) At 720 °C, ripening continues and graphene areas appear (dark, marked with arrows).

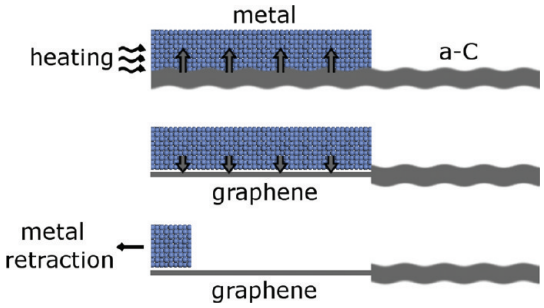

Figure 2. Schematic drawing of the growth process. Amorphous carbon (a-C) is taken up by the metal at high temperature. As soon as the bottom surface is uncovered, a graphene layer nucleates there. Retraction of the metal leaves a self-supporting graphene layer.

The segregation of graphenic carbon from the metal crystals was seen as a flat graphene layer in the trace of the migrating metal island but also in the shape of graphitic layers around the metal particles. In order to visualize the formation of graphene *in situ*, two procedures have been applied:

(1) As described above, annealing at temperatures above 600 °C leads to further ripening of the metal crystals. In the traces behind by the migrating metal islands, graphene layers become visible. The areas of the graphene layers as shown in Figure 1C were typically 0.01−0.02 μm^2.

(2) Electron irradiation of the edge of a metal island sitting on the amorphous carbon film leads to the growth of a thin metal layer above 500 °C, starting from the island and growing over the amorphous carbon. This effect is due to the beam-induced surface migration of metal atoms that become attached on top of the amorphous carbon layer at the edge of the metal island (J. A. Rodríguez *et al.*, manuscript in preparation). The metal growth follows the beam spot, which is moved slowly in a defined way to create a thin metal lamella on the amorphous carbon film. The inherent instability of such a metal lamella with increasing aspect ratio leads to a sudden retraction of the lamella toward the metal island after a certain length has been exceeded. The retraction can also be induced by increasing the temperature. At a sufficiently high temperature, the transformation of carbon can be seen on the trace of the retracting metal lamella. With this technique, graphene was obtained even below 600 °C, though of a rather defective nature. Typical graphene layers grown by this technique were 10−20 nm in width and 100−200 nm in length.

Figure 3 shows examples of graphene grown from Fe, Co, and Ni after heating-induced metal migration. The graphenic areas often show different crystallographic orientations, separated by defect boundaries (Figure 3B,C). Point defects such as vacancies are always present. Although some of them might have been created during growth, the majority are due to exposure to the electron beam (200 keV energy). Under the unavoidable electron irradiation in this *in situ* study, vacancies appeared and grew rapidly so that larger holes in the graphene layers appeared. This is a well-known irradiation effect occurring in graphenic structures when the electron energy exceeds the threshold for carbon atom displacements of approximately 80−90 keV.[29−31] Metal atoms, seen as dark spots, were also frequently observed on the graphene layers, pointing to the existence of a strong graphene−metal interaction which induces metal leaching onto the graphene during its growth.

The observations indicate that graphene layers grow on the whole surface of the metal and not only from the retracting edge. This became visible when contamination in the form of graphitic particles or metal atoms was located on the side of the graphene layers opposite to the metal. If the metal crystals were thin

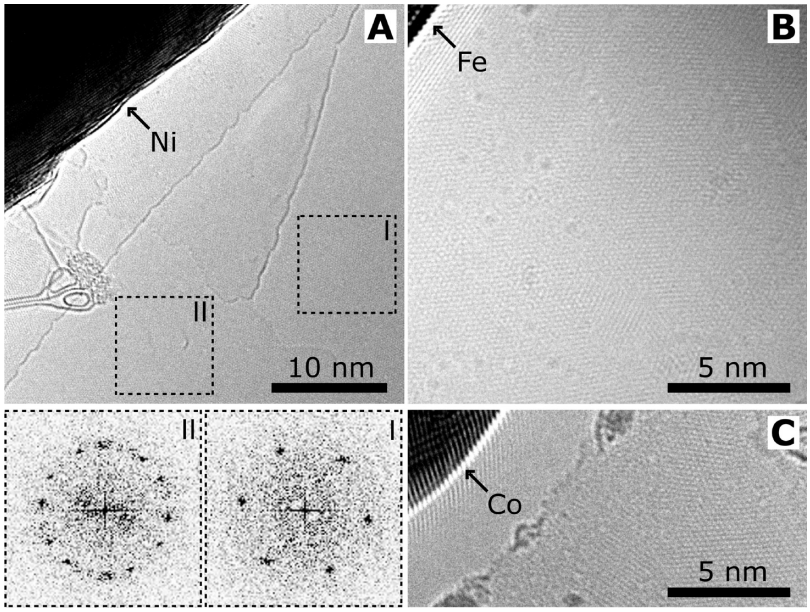

Figure 3. Graphene grown from Ni (A), Fe (B), and Co (C) crystals at 730, 680, and 640 °C, respectively. (A) Single- (I) and double-layer (II) graphene regions at the edge of a retracting Ni crystal. Diffractograms I and II (obtained by Fourier transformation from the dashed squares I and II) show the presence of a single layer (I) and a double layer (II), where the two planes are rotated by 25° relative to each other. (B) Few-layer graphene grown from Fe (visible in the upper left corner) showing vacancies and larger defects. (C) Graphene grown from Co. The annular hole around the metal was made intentionally with the electron beam to allow an estimation of the number of layers.

enough, the contaminants were already observable through the metal before but also after the metal had retracted. These contaminants do not change their position when the metal layer moves over them. An example is shown in Figure S1 and Video-S1 in the Supporting Information. Graphene growth from the retracting edge of the metal crystals can thus be excluded. Graphene growth occurs in many cases on both sides of the metal, that is, at the metal surface where the interface with the amorphous carbon film had initially been located, but also on the opposite side. No influence of the crystallographic orientation of the metal on the nucleation and growth of graphene was observed, thus epitaxial constraints can be excluded.

Figure 4 shows the growth and retraction of a metal lamella by electron irradiation (procedure 2). After retraction of the metal, the amorphous carbon layer has vanished and graphene is left, similar to the case of thermal migration of the metal. The beam-induced growth of the metal lamella has the experimental advantage that patterns of metal layers, and eventually patterns of graphene, can be created. Examples are shown for Ni (Figure 4A–C) and Co (Figure 4D–F). High-resolution imaging (Figure 4G) and diffractograms (inset below Figure 4F) show that the vacated traces are occupied by graphene, whereas the surrounding layer is still amorphous. The whole process of retraction of the metal lamella can be seen in Video-S2 of the Supporting Information. An impression from the dynamics of the process can be gained from another example in Video-S3.

To detect the presence of carbon in the metal layer during graphene growth, Figure 5 shows electron energy loss spectra (EELS) from a line scan of the electron beam across a Co lamella that grew over the amorphous carbon film under electron irradiation at 550 °C. A reference spectrum (RT) taken from the pristine metal–carbon bilayer system at room temperature, before an interaction took place, shows both the carbon and Co edges. Whereas pure carbon is detected on the uncovered amorphous carbon film (a, b, g), the carbon edge drops and eventually vanishes while the Co edge appears when the beam is moved across the Co lamella (c–f). This shows that the amorphous carbon has been taken up completely by the metal layer.

DISCUSSION

The segregation of graphitic carbon from carbon-doped transition metals has already been studied in the 1970s and 1980s, for example, in the growth of carbon layers on Ni[11] or on Co and other transition metals.[12] It has been found that a "surface monolayer" of carbon (which was presumably what we call graphene today) grows, for example, on Ni(111) surfaces in a range between a precipitation temperature T_p and a segregation temperature T_s. Below T_p, bulk graphite precipitates on the surface, whereas above T_s, the coverage of the surface is too low for a coherent carbon layer. These studies have already shown that graphene (although its structure was not characterized) grows after bulk diffusion of carbon in a metal and successive segregation. The growth of graphene in a solid-state process has also been shown in recent studies by STM,

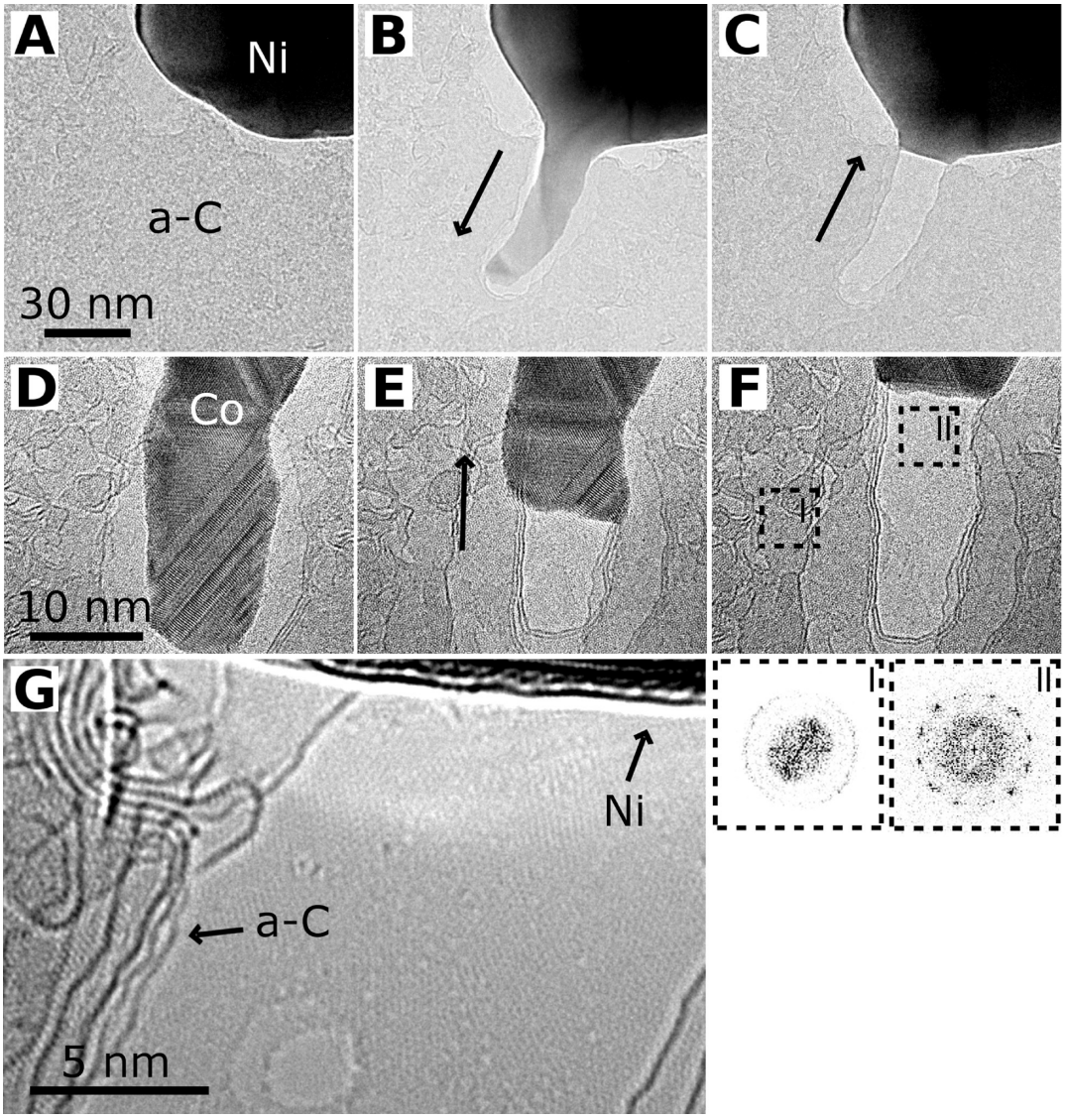

Figure 4. Growth and retraction of metal lamellae on amorphous carbon by electron irradiation and subsequent growth of graphene. (A) Ni crystal before generation of the lamella. (B) Lamella as created by electron irradiation. (C) Retraction of the lamella at 560 °C. (D−F) Retraction of a Co lamella at 640 °C at acquisition times of 1 (D), 159 (E), and 196 s (F) after formation of the lamella. A graphene layer is always left in the "fjord", where the lamella has retracted. Diffractograms from the amorphous surrounding film and the graphene layer in (F) are shown in the insets. (G) Double-layer graphene after retraction of a Ni lamella at 720 °C. Graphitic layers originating from carbon segregation on top of the Ni crystal are visible on the left-hand side. A hole in graphene (bottom) has intentionally been made with the electron beam to determine the number of layers.

for example, by transferring carbon atoms from HOPG through Ni crystals.[32]

The present study is widely in accordance with the early work. From our observations by imaging and EELS, it is clear that the amorphous carbon layer is taken up by the metal crystal at temperatures above 600 °C (Co, Ni) or 560 °C (Fe). Since amorphous carbon is metastable and thus an energetically higher modification of carbon, the barrier for diffusion into the metal should be lower than that for carbon atoms in the energetically more favorable modification of graphene. Overall, there is an energy gain when the system transforms from amorphous carbon with its unsaturated bonds to perfect graphene. Since the solubility of carbon in the metals is too low for an uptake of all carbon from the underlying film (*e.g.*, < 0.1 atom % C in Co at the highest temperature of this study[12,33]), we have to assume that most carbon atoms diffuse sideways and segregate at the edges of the metal crystals. Indeed, this is seen in the shape of disordered graphitic layers forming on and in the vicinity of some of the metal crystals (Figure 4G). This phenomenon is similar to what has been observed during carbon nanotube synthesis from metal catalysts where carbon precipitates on some specific surfaces of the particle to form the nanotube. In any case, it is obvious to assume that the metal crystals are saturated with carbon before the precipitation of graphene.[34] Once the amorphous carbon layer disappears from the interface, a graphene layer nucleates on the same

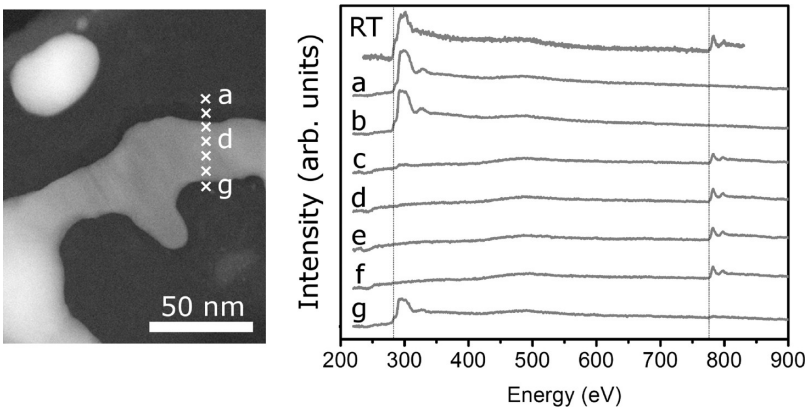

Figure 5. EELS from a line scan over a Co lamella grown by electron irradiation on an amorphous carbon film. The image on the left is a dark-field STEM image showing the Co layer in bright contrast. The spectrum labeled RT was taken from the pristine metal−carbon sample at room temperature before the interaction of Co with carbon. After the interaction at high temperature, seven spectra have been taken on the points labeled a−g. The spectra from the uncovered carbon film (a, b, g) show the carbon edge at 283 eV. Spectra taken from the area covered by the Co lamella show the Co edge at 779 eV but almost no trace of carbon.

surface of the metal crystal, but growth may happen on the other side, as well. It appears that a flat metal surface is necessary for graphene growth. Surface (respectively interface) steps may play a role during the nucleation of the graphene layer,[14,35] although these steps were not visible here.

Since graphene growth occurs at constant or even rising temperature, a nucleation due to cooling-induced supersaturation can be excluded. The solubility of carbon in the metal is important as the thickness of graphene (*i.e.*, the number of layers) increases with increasing solubility of carbon in the respective metal, that is, from Co over Ni to Fe. On Cu with its negligible solubility for carbon, no nucleation of graphene is observed. On Co, which has a low solubility for carbon, single-layer graphene was observed frequently, whereas Fe (high carbon solubility) produced rather multilayer graphene. (As a side note, we are not aware of other recent studies showing graphene growth from Fe crystals.) The thickness of the metal layer from where graphene grows might also play a certain role (*e.g.*, Fe formed thicker crystals than Co in our study). The diffusivity of carbon in all transition metals is fast (*e.g.*, 1.4×10^{-14} m^2 s^{-1} in Co at 600 °C[36]); therefore, we can exclude diffusion as a growth-limiting factor in this process. The metal crystals act as diffusion channels to transport carbon atoms rapidly to each location at the surface so that a continuous graphene layer segregates.

CONCLUSIONS

We have shown that graphene layers can be grown by dissolving amorphous carbon in catalytically active solid metals. The experimental advantage of this procedure is the possibility to observe the growth of graphene *in situ* at high resolution in an electron microscope. We can conclude that saturation of the metal with carbon and bulk diffusion of carbon in the metal precedes the nucleation and growth of graphene. The transformation from amorphous carbon to graphene is driven by a lowering of the energy of the system, while the reaction barrier for this transformation is lowered by the catalytically active metal. The growth temperature can be kept lower than in most other techniques of graphene growth (*e.g.*, from the gas phase). The rather high concentration of defects in graphene, such as tilt boundaries, that we observe in the present work could be avoided at higher growth temperatures and by using metals with a lower carbon solubility.

The technique of transforming amorphous carbon to graphene may find different applications in nanotechnology. Amorphous carbon can easily be evaporated on transition metal layers (the inverse of the preparation procedure in this study). After heating, the metal could be removed by etching so that free-standing graphene layers remain in preselected positions.

EXPERIMENTAL METHODS

Coherent polycrystalline films of Fe, Co, Ni, and Cu with thicknesses and crystallite sizes of approximately 10 nm (Co, Ni, and Cu) or 30 nm (Fe) were sputtered onto amorphous carbon films of approximately 20 nm in thickness spanning over the holes of Cu grids for electron microscopy. The metal deposition was carried out in a cathodic sputtering chamber with an Ar atmosphere (0.1 Pa) at room temperature. *In situ* electron microscopy of the samples was performed in the heating stage of a transmission electron microscope (JEOL 2100F, equipped with an aberration-corrected condenser and operated at 200 kV). Images were recorded with a CCD camera, and electron energy loss spectra (EELS) were taken with an imaging filter (Gatan). The evolution of the specimens as a

function of temperature was monitored *in situ* by increasing the temperature in small steps from room temperature to 730 °C.

Acknowledgment. Financial support by the Agence Nationale de Recherche (NANOCONTACTS, NT09 507527) is gratefully acknowledged. The authors thank M. Acosta and O. Cretu for assistance in sample preparation.

Supporting Information Available: Another image showing the growth of graphene from retracting metal islands is presented as well as an image series where the presence of graphene prior to the retraction of the metal is demonstrated. Three video sequences show the growth of graphene layers. This material is available free of charge *via* the Internet at http://pubs.acs.org.

REFERENCES AND NOTES

1. Geim, A. K. Graphene: Status and Prospects. *Science* **2009,** *324*, 1530–1534.
2. Castro Neto, A. H.; Guinea, F.; Peres, N. M. R.; Novoselov, K. S.; Geim, A. K. The Electronic Properties of Graphene. *Rev. Mod. Phys.* **2009,** *81*, 109–162.
3. Novoselov, K. S.; Geim, A. K.; Morozov, S. V.; Jiang, D.; Zhang, Y.; Dubonos, S. V.; Grigorieva, I. V.; Firsov, A. A. Electric Field Effect in Atomically Thin Carbon Films. *Science* **2004,** *306*, 666–669.
4. Novoselov, K. S.; Jiang, D.; Schedin, F.; Booth, T. J.; Khotkevich, V. V.; Morozov, S. V.; Geim, A. K. Two-Dimensional Atomic Crystals. *Proc. Natl. Acad. Sci. U.S.A.* **2005,** *102*, 10451–10453.
5. Van Bommel, A. J.; Crombeen, J. E.; Van Tooren, A. LEED and Auger Electron Observations of the SiC(0001) Surface. *Surf. Sci.* **1975,** *48*, 463–472.
6. Berger, C.; Song, Z.; Li, T.; Li, X.; Ogbazghi, A. Y.; Feng, R.; Dai, Z.; Marchenkov, A. N.; Conrad, E. H.; First, P. N.;*et al.* Ultrathin Epitaxial Graphite: 2D Electron Gas Properties and a Route toward Graphene-Based Nanoelectronics. *J. Phys. Chem. B* **2004,** *108*, 19912–19916.
7. Reina, A.; Jia, X.; Ho, J.; Nezich, D.; Son, H.; Bulovic, V.; Dresselhaus, M. S.; Kong, J. Large Area, Few-Layer Graphene Films on Arbitrary Substrates by Chemical Vapor Deposition. *Nano Lett.* **2009,** *9*, 30–35.
8. Li, X.; Cai, W.; An, J.; Kim, S.; Nah, J.; Yang, D.; Piner, R.; Velamakanni, A.; Jung, I.; Tutuc, E.;*et al.*Large-Area Synthesis of High-Quality and Uniform Graphene Films on Copper Foils. *Science* **2009,** *324*, 1312–1314.
9. Kim, K. S.; Zhao, Y.; Jang, H.; Lee, S. Y.; Kim, J. M.; Kim, K. S.; Ahn, J.-H.; Kim, P.; Choi, J.-Y.; Hong, B. H. Large-Scale Pattern Growth of Graphene Films for Stretchable Transparent Electrodes. *Nature* **2009,** *457*, 706–710.
10. Lee, Y.; Bae, S.; Jang, H.; Jang, S.; Zhu, S.-E.; Sim, S. H.; Song, Y. I.; Hong, B. H.; Ahn, J.-H. Wafer-Scale Synthesis and Transfer of Graphene Films. *Nano Lett.* **2010,** *10*, 490–493.
11. Eizenberg, M.; Blakely, J. M. Carbon Monolayer Phase Condensation on Ni(111). *Surf. Sci.* **1979,** *82*, 228–236.
12. Hamilton, J. C.; Blakely, J. M. Carbon Segregation to Single Crystal Surfaces of Pt, Pd and Co. *Surf. Sci.* **1980,** *91*, 199–217.
13. Qingkai, Y.; Jie, L.; Sujitra, S.; Hao, L.; Yong, P. C.; Shin-Shem, P. Graphene Segregated on Ni Surfaces and Transferred to Insulators. *Appl. Phys. Lett.* **2008,** *93*, 113103.
14. Sutter, P. W.; Flege, J.-I.; Sutter, E. A. Epitaxial Graphene on Ruthenium. *Nat. Mater.* **2008,** *7*, 406–411.
15. Pollard, A. J.; Nair, R. R.; Sabki, S. N.; Staddon, C. R.; Perdigao, L. M. A.; Hsu, C. H.; Garfitt, J. M.; Gangopadhyay, S.; Gleeson, H. F.; Geim, A. K.;*et al.*Formation of Monolayer Graphene by Annealing Sacrificial Nickel Thin Films. *J. Phys. Chem. C* **2009,** *113*, 16565–16567.
16. Ago, H.; Tanaka, I.; Orofeo, C. M.; Tsuji, M.; Ikeda, K. Patterned Growth of Graphene Over Epitaxial Catalyst. *Small* **2010,** *6*, 1226–1233.
17. Park, S.; Ruoff, R. S. Chemical Methods for the Production of Graphenes. *Nat. Nanotechnol.* **2009,** *4*, 217–224.
18. Kumar, M.; Yoshinori, A. Chemical Vapor Deposition of Carbon Nanotubes: A Review on Growth Mechanism and Mass Production. *J. Nanosci. Nanotechnol.* **2010,** *10*, 3739–3758.
19. Helveg, S.; Lopez-Cartes, C.; Sehested, J.; Hansen, P. L.; Clausen, B. S.; Rostrup-Nielsen, J. R.; Abild-Pedersen, F.; Norskov, J. K. Atomic-Scale Imaging of Carbon Nanofibre Growth. *Nature* **2004,** *427*, 426–429.
20. Sharma, R.; Iqbal, Z. *In Situ* Observations of Carbon Nanotube Formation Using Environmental Transmission Electron Microscopy. *Appl. Phys. Lett.* **2004,** *84*, 990–992.
21. Lin, M.; Ying Tan, J. P.; Boothroyd, C.; Loh, K. P.; Tok, E. S.; Foo, Y.-L. Direct Observation of Single-Walled Carbon Nanotube Growth at the Atomistic Scale. *Nano Lett.* **2006,** *6*, 449–452.
22. Rodriguez-Manzo, J. A.; Terrones, M.; Terrones, H.; Kroto, H. W.; Sun, L.; Banhart, F. *In-Situ* Nucleation of Carbon Nanotubes by the Injection of Carbon Atoms into Metal Particles. *Nat. Nanotechnol.* **2007,** *2*, 307–311.
23. Hofmann, S.; Sharma, R.; Ducati, C.; Du, G.; Mattevi, C.; Cepek, C.; Cantoro, M.; Pisana, S.; Parvez, A.; Cervantes-Sodi, F.;*et al. In-Situ* Observations of Catalyst Dynamics during Surface-Bound Carbon Nanotube Nucleation. *Nano Lett.* **2007,** *7*, 602–608.
24. Lin, M.; Tan, J. P. Y.; Boothroyd, C.; Loh, K. P.; Tok, E. S.; Foo, Y.-L. Dynamical Observation of Bamboo-like Carbon Nanotube Growth. *Nano Lett.* **2007,** *7*, 2234–2238.
25. Yoshida, H.; Takeda, S.; Uchiyama, T.; Kohno, H.; Homma, Y. Atomic-Scale *In-Situ* Observation of Carbon Nanotube Growth from Solid State Iron Carbide Nanoparticles. *Nano Lett.* **2008,** *8*, 2082–2086.
26. Rodríguez-Manzo, J. A.; Janowska, I.; Pham-Huu, C.; Tolvanen, A.; Krasheninnikov, A. V.; Nordlund, K.; Banhart, F. Growth of Single-Walled Carbon Nanotubes from Sharp Metal Tips. *Small* **2009,** *5*, 2710–2715.
27. Hannon, J. B.; Tromp, R. M. Pit Formation During Graphene Synthesis on SiC(0001): *In-Situ* Electron Microscopy. *Phys. Rev. B* **2008,** *77*, 241404.
28. Ohring, M. *The Materials Science of Thin Films*; Academic Press: London, 1991.
29. Hashimoto, A.; Suenaga, K.; Gloter, A.; Urita, K.; Iijima, S. Direct Evidence for Atomic Defects in Graphene Layers. *Nature* **2004,** *430*, 870–873.
30. Krasheninnikov, A. V.; Banhart, F. Engineering of Nanostructured Carbon Materials with Electron or Ion Beams. *Nat. Mater.* **2007,** *6*, 723–733.
31. Meyer, J. C.; Kisielowski, C.; Erni, R.; Rossell, M. D.; Crommie, M. F.; Zettl, A. Direct Imaging of Lattice Atoms and Topological Defects in Graphene Membranes. *Nano Lett.* **2008,** *8*, 3582–3586.
32. Murata, Y.; Petrova, V.; Kappes, B. B.; Ebnonnasir, A.; Petrov, I.; Xie, Y.-H.; Ciobanu, C. V.; Kodambaka, S. Moiré Superstructures of Graphene on Faceted Nickel Islands. *ACS Nano* **2010,** *4*, 6509–6514.
33. Hasebe, M.; Ohtani, H.; Nishizawa, T. Effect of Magnetic Transition on Solubility of Carbon in bcc Fe and fcc Co-Ni Alloys. *Metall. Trans. A* **1985,** *16*, 913–921.
34. Deck, C. P.; Vecchio, K. Prediction of Carbon Nanotube Growth Success by the Analysis of Carbon-Catalyst Binary Phase Diagrams. *Carbon* **2006,** *44*, 267–275.
35. Saadi, S.; Abild-Pedersen, F.; Helveg, S.; Sehested, J.; Hinnemann, B.; Appel, C. C.; Norskov, J. K. On the Role of Metal Step-Edges in Graphene Growth. *J. Phys. Chem. C* **2010,** *114*, 11221–11227.
36. McLellan, R. B.; Ko, C.; Wasz, M. L. The Diffusion of Carbon in Solid Cobalt. *J. Phys. Chem. Solids* **1992,** *53*, 1269–1273.